

Photoionization of the Fe Ions: Structure of the K-Edge

P. Palmeri*, C. Mendoza*, T. Kallman* and M. Bautista†

*Laboratory for High Energy Astrophysics, NASA Goddard Space Flight Center, Greenbelt MD 20771, USA

†Centro de Física, IVIC, Caracas 1020A, Venezuela

Abstract. X-ray absorption and emission features arising from the inner-shell transitions in iron are of practical importance in astrophysics due to the Fe cosmic abundance and to the absence of traits from other elements in the nearby spectrum. As a result, the strengths and energies of such features can constrain the ionization stage, elemental abundance, and column density of the gas in the vicinity of the exotic cosmic objects, e.g. active galactic nuclei (AGN) and galactic black hole candidates. Although the observational technology in X-ray astronomy is still evolving and currently lacks high spectroscopic resolution, the astrophysical models have been based on atomic calculations that predict a sudden and high step-like increase of the cross section at the K-shell threshold (see for instance Ref. [1]).

New Breit-Pauli R-matrix calculations of the photoionization cross section of the ground states of Fe XVII in the region near the K threshold are presented. They strongly support the view that the previously assumed sharp edge behaviour is not correct. The latter has been caused by the neglect of spectator Auger channels in the decay of the resonances converging to the K threshold. These decay channels include the dominant KLL channels and give rise to constant widths (independent of n). As a consequence, these series display damped Lorentzian components that rapidly blend to impose continuity at threshold, thus reformatting the previously held picture of the edge. Apparent broadened iron edges detected in the spectra of AGN and galactic black hole candidates seem [2, 3] to indicate that these quantum effects may be at least partially responsible for the observed broadening.

INTRODUCTION

X-ray absorption and emission features due to inner shell transitions in iron are of practical importance in astronomy, owing to the cosmic abundance of iron and to the absence of features from other elements nearby in the spectrum. As a result, the strengths and energies of iron K shell features can constrain the ionization state, elemental abundance, and column density of gas in the vicinity of exotic objects such as active galactic nuclei (AGN) and galactic black hole candidates. Although the observational technology in X-ray astronomy is still evolving, many such features have been observed. Emission lines have been used to constrain the geometrical distribution of gas in compact binary stars [4], and to detect black holes in AGN [5]. Iron absorption features have been detected from AGN [6], from compact binaries [7], and from galactic black hole candidates [8, 3]. These divide naturally into bound-bound and bound-free transitions, and much of the interpretation of the bound-free absorption features has been based on atomic calculations such as those of Verner and Yakovlev [9] or Berrington and Ballance [1] which predict

a sudden increase in the cross section at the binding energy of the K-shell electron.

When a photon is sufficiently energetic to promote a K-shell electron to a higher Rydberg state, the resulting excited state can decay via Auger channels. In the case of Fe XVII, we have these possible decay pathways:

$$\begin{aligned}
 h\nu + 2p^6 &\rightarrow 1s^{-1}2p^6np \\
 &\rightarrow \left\{ \begin{array}{l} 2p^5 + e^- \\ 2s^{-1}2p^6 + e^- \end{array} \right\} \quad (1)
 \end{aligned}$$

$$\rightarrow \left\{ \begin{array}{l} 2p^4np + e^- \\ 2s^{-1}2p^5np + e^- \\ 2s^{-2}2p^6np + e^- \end{array} \right\} \quad (2)$$

Eq. (1) represents the participator (KL*n*) channels where the *np* Rydberg electron is involved in the decay while it is not in the spectator (KLL) channels (Eq. (2)). R-matrix calculations have been carried out to analyze the role of the spectator channels.

In the following sections, we will detail the methodology and discuss the results.

THEORY

The Breit-Pauli R-matrix method (BPRM) is widely used in electron-ion scattering and in radiative bound-bound and bound-free calculations. It is based on the close-coupling approximation [10] whereby the wavefunctions for states of an *N*-electron target and a colliding electron with total angular momentum and parity *Jπ* are expanded in terms of the target eigenfunctions

$$\Psi^{J\pi} = \mathcal{A} \sum_i \chi_i \frac{F_i(r)}{r} + \sum_j c_j \Phi_j \quad (3)$$

The functions χ_i are vector coupled products of the target eigenfunctions and the angular part of the incident-electron functions, $F_i(r)$ are the radial part of the latter and \mathcal{A} is an antisymmetrization operator. The functions Φ_j are bound-type functions of the total system constructed with target orbitals; they are introduced to compensate for orthogonality conditions imposed on the $F_i(r)$ and to improve short-range correlations. The Kohn variational method gives rise to a set of coupled integro-differential equations that are solved by R-matrix techniques [11, 12] within a box of radius, say, $r \leq a$. In the asymptotic region ($r > a$), solutions are found using the MQDT method [15, 16]. Breit-Pauli relativistic corrections have been introduced in the R-matrix suite by Scott and Burke [13], Scott and Taylor [14]. Inter-channel coupling is equivalent to configuration interaction in the atomic structure context, and presents a formal and unified approach to study the decay properties of both bound states and resonances.

STRATEGY

In order to display the different effects of these two types of Auger decays, two calculations of the photoionization cross section have been carried out (hereafter referred to as Calculations A and B). In Calculation A, the BPRM method have been used to solve the $e^- + \text{Fe}^{17+}$ system. The following target configurations were considered: $2p^5$, $2s^{-1}2p^6$, and $1s^{-1}2p^6$. Only the participator Auger channels described in Eq.(1) were therefore included. The orbitals of the target ion were optimized using the code SUPERSTRUCTURE [17]. As it was obviously impossible to include all the $2p^4np$, $2s^{-1}2p^5np$, and $2s^{-2}2p^6np$ target configurations in our R-matrix model, Calculation B was carried out in two steps. Firstly, an R-matrix calculation was carried out adding the contributions of KLL Auger decays of the $1s^{-1}2p^63p$ resonances (Eq.(2)). The next step consisted in fitting Lorentzian profiles to these 3p resonances in order to obtain the widths and areas. These symmetric profiles are due to the dominance of the KLL channels over the KLn ones. Actually, these spectator Auger channels produce continuum states that cannot be reached by direct photoionization of the ground state causing the Fano q parameter to go to infinity (see Nayandin et al. [18] and references therein). As the Auger rates of the spectator channels are constant along the Rydberg series, the cross section was extrapolated for the higher members of the series using Lorentzian profiles with a constant width and areas decreasing as the third power of the effective quantum number, n^* . The resonance positions were deduced by the usual Ritz formula using the data of Calculation A.

RESULTS AND DISCUSSION

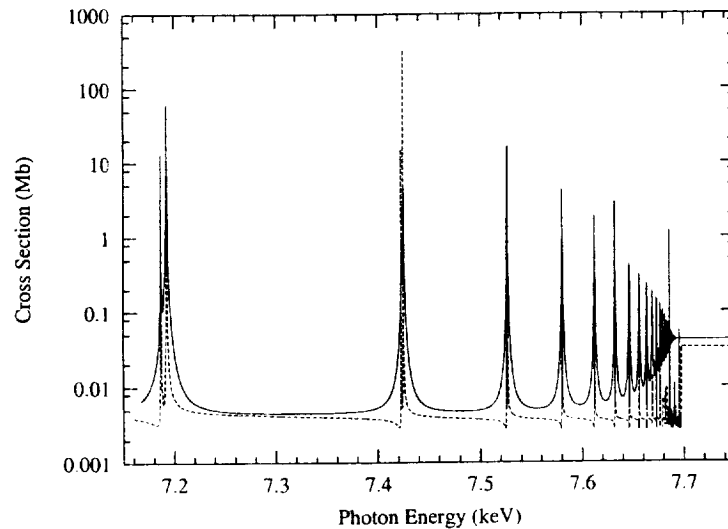


FIGURE 1. Total photoionization cross section in Mb versus photon energy in keV. Solid and dash lines are Calculations B and A respectively (see the text). The sharp K-edge near 7.7 keV in Calculation A has disappeared in Calculation B.

In Fig. 1, a comparison between Calculation A and B is shown. The sharp K-edge near 7.7 keV has disappeared, being filled up by the highest members of the Rydberg series which are blended together. Note also the differences in the resonance shapes and intensities. Because of the constant width, the intensities decrease as $1/(n^*)^3$ in Calculation B. In Table 1, a comparison between widths obtained by two R-matrix calculations (with and without the spectator Auger channels) is presented for the 3p and 4p resonances. One can see the significant effect of the spectator (KLL) Auger decays on the widths. As the KLn widths (Γ^{KLn}) are going down as $(n^*)^{-3}$ and the KLL ones are independent of n^* , the resulting widths ($\Gamma^{KLn+KLL}$) become constant for the highest members of the Rydberg series. Actually, see Table 1, we can conclude that they are almost constant for the first few members.

TABLE 1. Comparison between widths obtained without (Γ^{KLn}) and with the KLL (spectator) Auger decays ($\Gamma^{KLn+KLL}$) using the BPRM method for the 3p and 4p resonances.

Resonance	E (keV)	Γ^{KLn} (eV)	$\Gamma^{KLn+KLL}$ (eV)
$1s^{-1}2p^63p^3P_1^o$	7.1865	3.802×10^{-2}	6.495×10^{-1}
$1s^{-1}2p^63p^1P_1^o$	7.1923	2.165×10^{-2}	6.335×10^{-1}
$1s^{-1}2p^64p^3P_1^o$	7.4224	1.386×10^{-2}	6.146×10^{-1}
$1s^{-1}2p^64p^1P_1^o$	7.4246	7.952×10^{-3}	6.082×10^{-1}

Fig. 2 depicts the cross section obtained in Calculation B convoluted with an instrumental (Gaussian) profile of 10 eV. The ‘edge’ is now shifted down to 7.6 keV. The 9p resonances are the highest resolved member of the Rydberg series. Unfortunately, we have found no experimental data in Fe XVII to compare with our calculations. Nevertheless, Farhat et al. [19] have measured the total electron yield of the $h\nu + 3p^6 \rightarrow 2p^{-1}3p^6 + e^-$ photoionization process in neutral argon. The $2p^{-1}3p^6nl$ resonances can decay via dominant spectator Auger channels to the $3p^4nl$, $3p^{-1}3p^5nl$, and $3s^{-2}3p^6nl$ Ar II configurations. Fig. 3 is the reprint of Fig. 2 in Farhat et al. [19] which presents the total electron yield versus photon energy (the resolution is 160 meV). The $2p_{3/2}$ threshold is indicated at 248.6 eV but no sharp edge is seen at this energy. Note the similar behaviour near threshold with Fig. 2. Actually, Gorczyca and Robicheaux [20] used an optical potential within the MQDT method to mimic the effect of the spectator Auger channels on the L-shell photoionization cross section of neutral argon. This technique has been also compared to measurements of the total electron yield near the K-shell threshold in neutral neon [21] and oxygen [22].

The calculations presented here show that the K-shell photoabsorption cross section for Fe XVII does not exhibit a sharp edge at the the binding energy of the K-shell electron, but it is shifted and broadened towards lower energies. It is worth pointing out that apparently broadened iron edges have been detected in the spectra of AGN and galactic black hole candidates [2, 3], and the same physical processes we identify here may be at least partially responsible for the observed broadening.

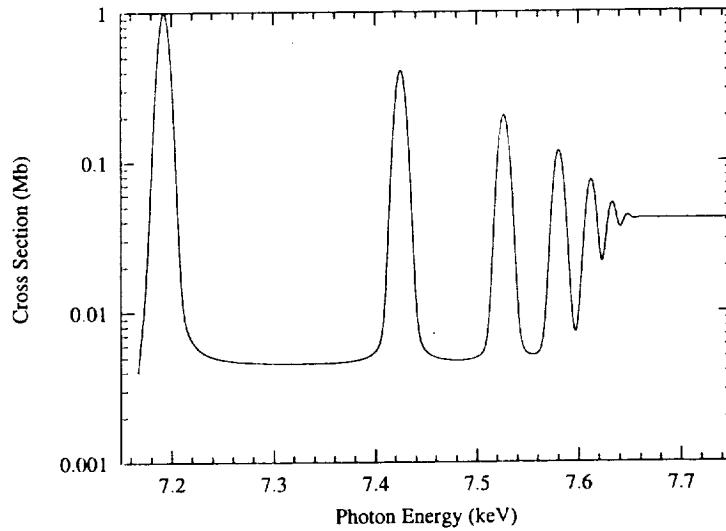


FIGURE 2. Total cross section obtained in Calculation B (see the text) convoluted with a Gaussian profile with a width of 10 eV.

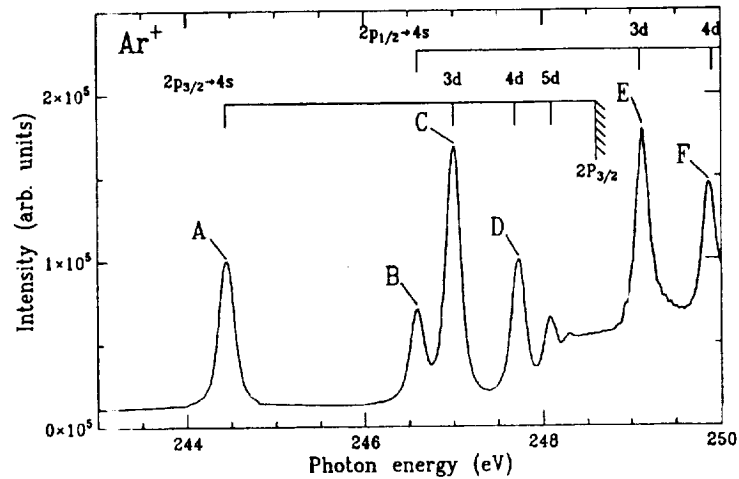


FIGURE 3. Total electron yield versus photon energy in eV as measured in Ar I by Farhat et al. [19]. The energy scan was taken over the $2p^{-1}nl$ resonances.

CONCLUSION

As an important conclusion, this work shows that the sharp edge structures at thresholds disappear when the Rydberg series before threshold are affected by spectator Auger decays. These inner-shell Auger channels cause constant-width Lorentzian shape resonances that blend near the threshold changing drastically the structure of the edge. Although this effect has been measured for the L-edge in neutral argon and for the K-shell in neutral neon and oxygen, experimental data are needed for the K-edge in Fe XVII.

ACKNOWLEDGMENTS

CM and PP kindly acknowledge a Senior Research Associateship from the National Research Council and a Research Associateship from University of Maryland respectively.

REFERENCES

1. Berrington, K. A., and Ballance, C. P., *J. Phys. B* **34**, 2697-2705 (2001).
2. Done, C., and Zycki, P., *Mon. Not. R. Astron. Soc.* **305**, 457-468 (1999).
3. Miller, J. M., Fabian, A. C., Wijnands, R., Remillard, R. A., Wojdowski, P., Schulz, N. S., Di Matteo, T., Marshall, H. L., Canizares, C. R., Pooley, D., and Lewin, W. H. G., *Astrophys. J.*, in press (2002).
4. Ebisawa, K., Day, C. S. R., Kallman, T. R., Nagase, F., Kotani, T., Kawashima, K., Kitamoto, S., and Woo, J. W., *Publ. Astron. Soc. Jpn* **48**, 425-440 (1996).
5. Tanaka, Y., Nandra, K., Fabian, A. C., Inoue, H., Otani, C., Dotani, T., Hayashida, K., Iwasawa, K., Kii, T., Kunieda, H., Makino, F., and Matsuoka, M., *Nature* **375**, 659-661 (1995).
6. Nandra, K., Pounds, K. A., Stewart, G. C., Fabian, A. C., and Rees, M. J., *Mon. Not. R. Astron. Soc.* **236**, 39P-46P (1989).
7. Shulz, N., and Brandt, N., *Astrophys. J.*, in press (2002).
8. Kotani, T., Ebisawa, K., Dotani, T., Inoue, H., Nagase, F., Tanaka, Y., and Ueda, Y., *Astrophys. J.* **539**, 413-423 (2000).
9. Verner, D., and Yakovlev, D. G., *Astron. Astrophys. Suppl. Ser.* **109**, 125-133 (1995).
10. Burke, P. G., and Seaton, M. J., *Meth. Comput. Phys.* **10**, 1 (1971).
11. Burke, P. G., Hibbert, A., and Robb, D., *J. Phys. B* **4**, 153-161 (1971).
12. Berrington, K. A., Burke, P. G., Butler, K., Seaton, M. J., Storey, P. J., Taylor, K. T., and Yan, Yu., *J. Phys. B* **20**, 6379-6397 (1987).
13. Scott, N. S., and Burke, P. G., *J. Phys. B* **12**, 4299-4314 (1980).
14. Scott, N. S., and Taylor, K. T., *Comput. Phys. Commun.* **25**, 347-387 (1982).
15. Seaton, M. J., *Proc. Phys. Soc. London* **88**, 801-814 ; 815-832 (1966).
16. Seaton, M. J., *Rep. Prog. Phys.* **46**, 167-257 (1983).
17. Eissner, W., Jones, M., and Nussbaumer, N., *Comput. Phys. Commun.* **8**, 270-306 (1974).
18. Nayandin, O., Gorczyca, T. W., Wills, A. A., Langer, B., Bozek, J. D., and Berrah, N., *Phys. Rev. A* **64**, 022505 (2001).
19. Farhat, A., Humphrey, M., Langer, B., Berrah, N., Bozek, J. D., and Cubaynes, D., *Phys. Rev. A* **56**, 501-513 (1997).
20. Gorczyca, T. W. and Robicheaux, F., *Phys. Rev. A* **60**, 1216-1225 (1999).
21. Gorczyca, T. W., *Phys. Rev. A* **61**, 024702 (2000).
22. Gorczyca, T. W. and McLaughlin, B. M., *J. Phys. B* **33**, L859-L863 (2000).